Economic Geology
Vol. 88, 1993, pp. 377–396

Formation of Massive Sulfide Lenses by Replacement of Folds: The Hercules Pb-Zn Mine, Tasmania

DOMINGO G. A. M. AERDEN*

Geology Department, James Cook University of North Queensland, Townsville, Queensland 4811, Australia

Abstract

The Hercules Pb-Zn deposit consists of a number of isolated, ellipsoidal massive sulfide pods hosted in a tuffaceous slate unit of Middle Cambrian age. These pods are aligned roughly parallel to the main cleavage and have completely discordant to moderately folded bedding. Mineralization is localized in the short limb zones of parasitic F_2 folds from the micro- to the macroscopic scale. Antithetic shearing induced along the bedding during D_3 caused localized dilation and fracturing of some of the short limb zones. This resulted in alteration and replacement late in D_3 such that S_3 was overprinted by the mineralization. The following paragenetic replacement sequence exists: pyrite I → quartz → chlorite → pyrite II → (sphalerite-galena-chalcopyrite). Pb isotope age data are consistent with the derivation of the deposit from dispersed primary sulfides in the Mount Read Volcanics by synmetamorphic mobilization into structural traps at higher levels in the crust.

Introduction

THE Mount Read Volcanics of western Tasmania consist of felsic lavas, pyroclastics, and volcano-sedimentary units that form the eastern side of a north-south–trending Cambrian basin known as the Dundas trough (Fig. 1). The volcanic belt is an important metallogenic province and hosts two different types of orebodies (Corbett, 1981, 1986; Solomon, 1981; Collins and Williams, 1986; Corbett et al., 1989). One type comprises Devonian granite-related, Sn-W replacement and vein deposits, and the second type consists of Cu-Pb-Zn massive sulfide deposits that are generally regarded as being of Cambrian volcanogenic (pretectonic) origin. Among the largest of the Cu-Pb-Zn deposits are the Rosebery, Mount Lyell, Hellyer, Que River, and Hercules orebodies.

The Hercules deposit occurs in a narrow, fine-grained metasedimentary horizon within the massive, dacitic to rhyolitic "Central volcanic sequence" (Central volcanic belt) of the Mount Read Volcanics (Corbett, 1981, 1986; Corbett and Lees, 1987). The deposit, situated on the western slope of Mount Hamilton (2 km west of Mount Read; Figs. 1 and 2), was discovered in 1897 and mined between 1900 and 1985. No access to the underground workings is possible, but there is good exposure of the ore and host rock in road cuttings and several small open cuts and cone-shaped surface pits above the underground workings.

In plan and section, the orebody occurs as a series of isolated ore lenses that crosscut the bedding in the host rocks (Figs. 3, 4a and b). The discordant nature of the deposit led early investigators to conclude that the orebody formed syntectonically and was structurally controlled (Hall et al., 1954, 1965). However, following subsequent volcanogenic interpretations for the Rosebery and Mount Lyell ore deposits (Markham, 1968; Brathwaite, 1969; Solomon et al., 1969; Cox, 1981; Green, 1983; Green et al., 1981), the Hercules deposit was reinterpreted as a strongly deformed volcanogenic deposit (Burton, 1975; Green, 1986, 1990; Eastoe et al., 1987).

Structural and microstructural analysis in the Rosebery mine (Aerden, 1991, 1992) supports a syntectonic origin for the Rosebery orebody. Aerden presents evidence for the emplacement of mineralization by metasomatic replacement of the host rock, at sites controlled by foliation boudinage, and suggests that Cambrian sulfides from the volcanic pile were dissolved, transported upward, and redeposited in a structural trap during Devonian deformation-metamorphism. The findings at Rosebery provide the impetus for reconsidering the origin of the other massive sulfide deposits in the Mount Read Volcanics, as a common origin can be expected on the basis of similar mineralization style and isotopic signature (Gulson and Porritt, 1987; Solomon et al., 1988).

This paper presents structural relationships between the Hercules ore and the host rock. These relationships indicate syntectonic emplacement of the orebody. Approximately coeval emplacement with the Rosebery deposit is postulated.

Mine Geology

The ore lenses are hosted in an east-dipping tuffaceous sediment horizon within intermediate lavas and pyroclastics of the Central sequence of the

* Present address: Laboratoire de Tectonique et Géochronologie, Université de Sciences et Techniques du Langedoc, Place E. Bataillon, 34060 Montpellier Cédex, France.

0361-0128/93/1436/377-20$4.00

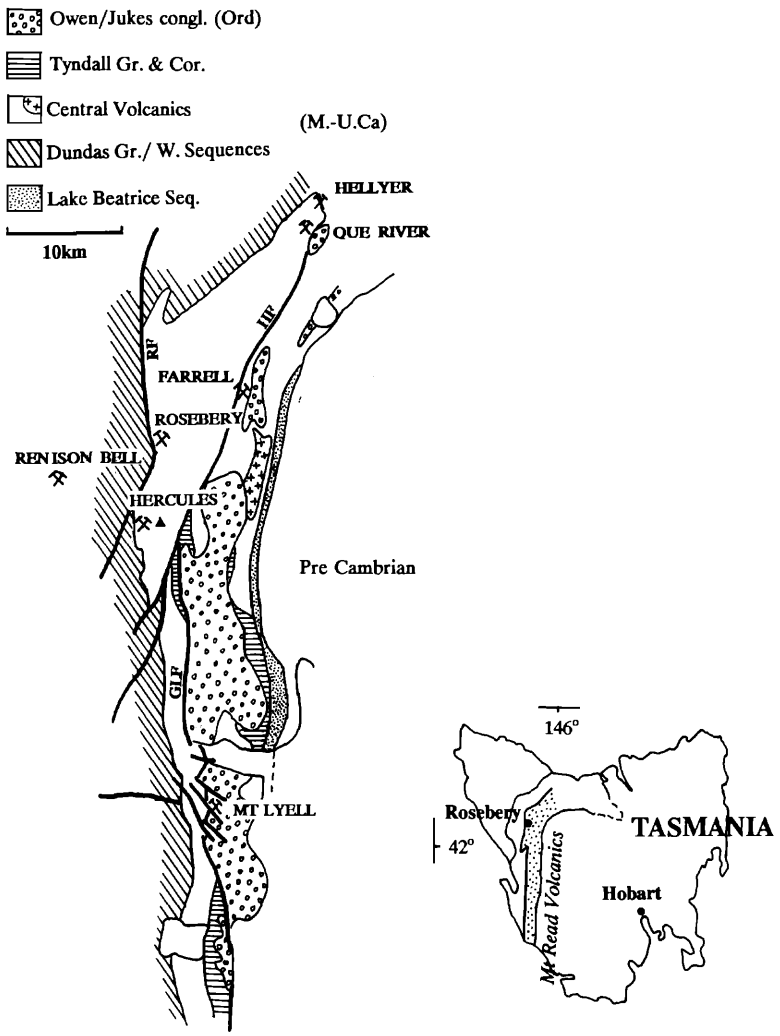

FIG. 1. The Cambrian Mount Read volcanic belt, including major Cu-Pb-Zn massive sulfide deposits. Renison Bell, just outside the Central volcanic belt, is an Sn deposit.

Mount Read Volcanics (Figs. 1 and 2). Wall-rock alteration associated with the orebody is developed both stratigraphically below and above the host rock in the volcanic units. In the immediate surroundings of the ore lenses, the slate is pale yellow due to intense leaching and sericitization (Fig. 2). In the lower parts of the slate unit, patches of intense chloritization are associated with disseminated mineralization.

Bedding layers could be traced continuously from zones of dark, little altered, tuffaceous slate into zones of strongly altered, sericite schist near the ore lenses (Fig. 4b). Thus, the slate and sericite schists appear to represent differentially altered parts of the same fine-grained tuffaceous sedimentary unit. Previously, the pale sericite schist zone hosting the ore was not recognized as the intensely altered equivalent of the Black Slate. This is why the distribution of the Black Slate does not accord with the bedding structure (Figs. 3a and 4a).

The footwall and hanging wall to the deposit consist of siliceous, feldspar phenocryst-bearing lavas and pyroclastics. These rocks have been altered to sericite-quartz-chlorite-epidote-carbonate assemblages and contain an anastomosing cleavage of variable intensity (Green et al., 1981; Allen and Cas, 1990). The original contact between the slate and the underlying volcanics is partially obliterated but roughly coincides with the transition from sericite-chlorite alteration to silica-dominated alteration in the footwall volcanics. Local intense silicification in narrow zones of intense anastomosing cleavage resulted in a lithology named "quartz-augen schist" by

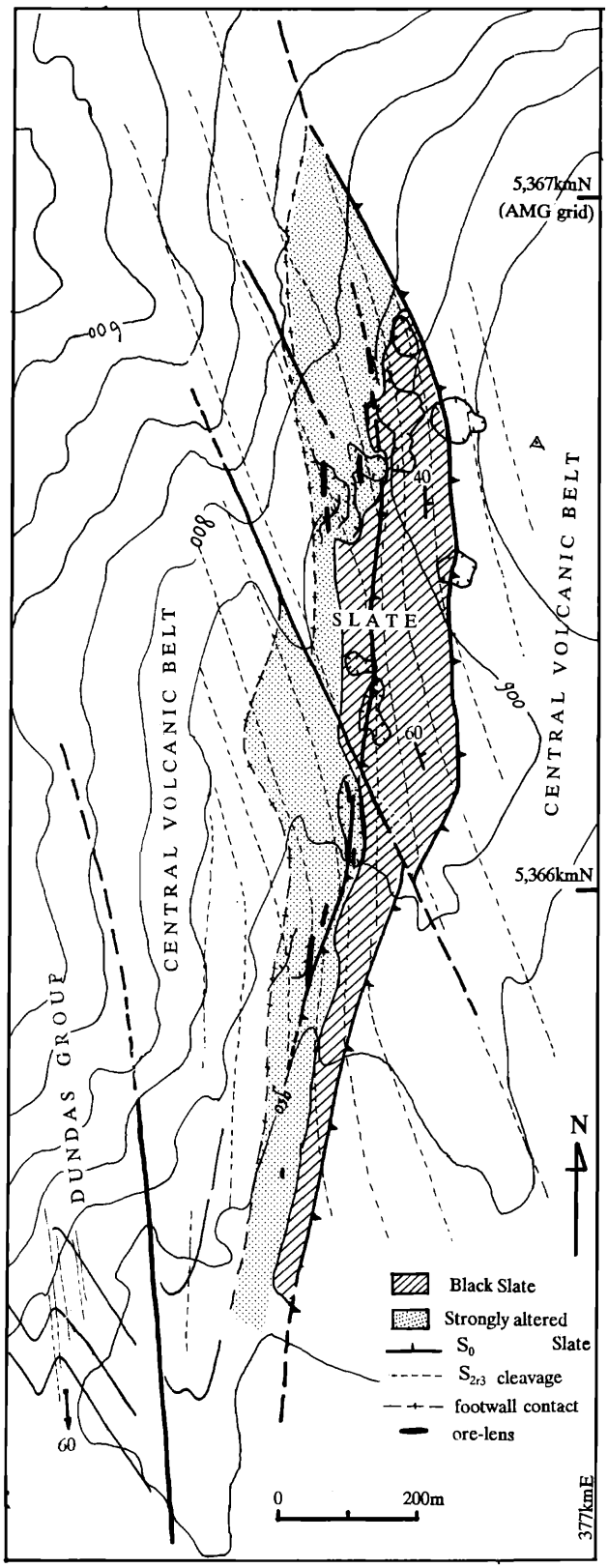

previous mine geologists and researchers. The hanging-wall contact between slate and volcanics is faulted and marked by an unmineralized fault breccia, up to 3 m wide.

Alteration and Metamorphism

The wall-rock alteration at Hercules is part of a regional alteration system in the Mount Read Volcanics that is associated with and intensifies near the massive sulfide deposits. This alteration produced Na, Ca, and Sr depletion and K, Fe, Mg, Ba, Rb, and H_2O enrichment in the volcanics (Green et al., 1981; Walshe and Solomon, 1981). Texturally, the alteration is expressed by the growth of quartz, sericite, chlorite, carbonate, and epidote and the destruction of feldspar phenocrysts.

Green et al. (1981), Hendry (1981), McLeod and Stanton (1984), and Eastoe et al. (1987) found that within the Rosebery and Mount Lyell orebodies, variations in the Fe-Mg content of chlorite correlated with mineralogical zoning patterns and variation of sulfur isotope values, indicating that wall-rock alteration was cogenetic with sulfide formation. It was recognized by some (e.g., Cox, 1981) that the alteration assemblages had grown syntectonically, but this was ascribed to recrystallization and solution-reprecipitation of an identical pretectonic alteration assemblage. However, microstructural evidence was not presented to support this assumption, whereas evidence supporting syntectonic wall-rock alteration has been presented by Aerden (1992) at Rosebery. Walshe and Solomon (1987) calculated from the mineral assemblages and chlorite compositions that regional metamorphic temperatures had been similar to the temperatures of the ore fluids. The regional alteration-metamorphic assemblages have been locally overprinted by a slightly higher grade, contact metamorphic assemblage (biotite-garnet-fluorite-K feldspar - quartz - tourmaline - pyrrhotite - magnetite-bornite, and chalcopyrite) associated with late tectonic, Devonian granite intrusions (Solomon et al., 1987).

Structural Development

Structural mapping at Hercules revealed a macroscopic structure of doubly plunging, parasitic folds in a dominantly east-dipping host-rock sequence (Figs. 3 and 4a). Mesoscopic fold geometries in bedding

FIG. 2. Geologic map of the mine area. The contact between the Central volcanic belt and the Dundas Group is a steeply dipping fault. The slate unit has been differentiated in a relatively unaltered part (Black Slate) and a part that is strongly sericitized (strongly altered slate). Outcropping ore is indicated in black.

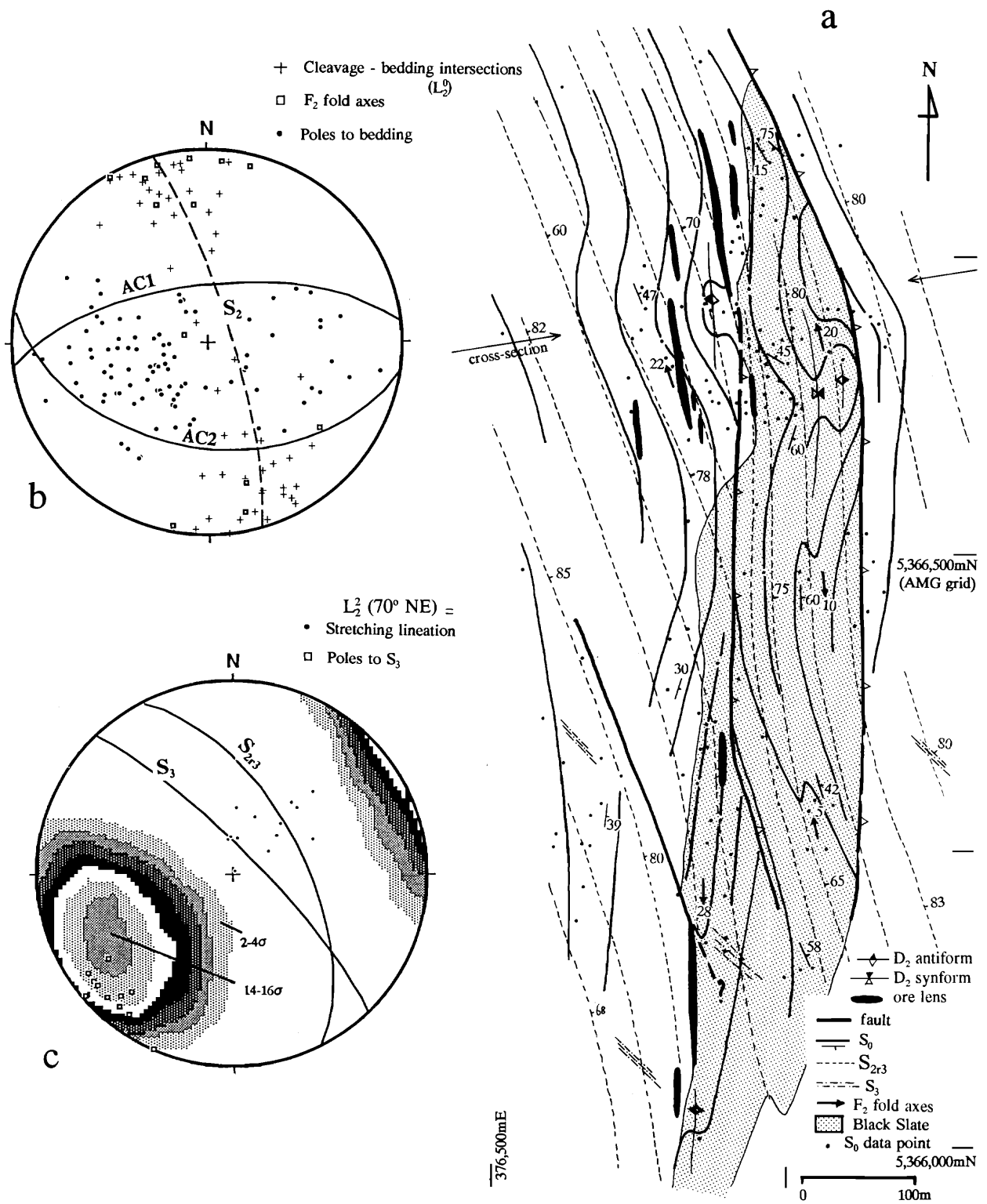

FIG. 3. a. Structural surface map of the central and northern mine area. The projected ore lenses are completely discordant to doubly plunging F_2^0 folds. The position of the cross section of Figure 4a is indicated by an arrow. b. F_2^0 fold axes and L_2^0 intersection lineations are doubly plunging and lie in a plane (dashed line), which is the average orientation of S_2. Poles to bedding (dots) lie on a fan of AC planes (perpendicular to variably plunging fold axes) between AC1 and AC2. c. Point density contours for S_2 and S_{2r3} measurements (3σ = uniform distribution). The average intersection lineation of S_3 and S_{2r3} (L_3^2) plunges gently south-southeast and the stretching lineations (L_2^2) on S_{2r3} plunge steeply northwest, approximately at right angles to L_3^2.

(S_0) are disharmonic and fold hinges die out rapidly so that the folds commonly appear isolated.

A regionally developed, second generation cleavage (S_2) at Hercules dips moderately to steeply east and strikes north-northwest–south-southeast. Relics of an S_1 foliation were only recognized in the strain shadows of porphyroclasts and it is uncertain whether they represent a true tectonic foliation or a bedding-parallel fissility. No mesoscopic evidence for pre-D_2 deformation was found.

An uncommon, weakly developed, subvertical, northwest-southeast–trending cleavage was observed in the field. In thin section it comprises a crenulation cleavage (S_3). In both horizontal and vertical east-west thin sections, F_3^2 crenulations have a "Z" asymmetry (looking south), indicating south-plunging crenulation axes and a shear sense along S_3 of the east block north and downward (Bell and Johnson, 1992).

The L_3^2 intersection lineations plunge approximately 20° to the south while the L_2^2 stretching lineation pitches 70° NE on the S_2 cleavage planes (Fig. 3a and b). The average orientation of the F_2^0 fold axes approximately parallels L_3^2.

Commonly, S_3 and crenulated S_2 are only preserved adjacent to rigid objects, such as pyrite porphyroblasts, volcanic feldspars, or early veins, whereas an intense planar S_2 fabric dominates the matrix away from the heterogeneities (Fig. 5a and b). S_2 appears to be progressively decrenulated, whereas S_3 becomes obliterated as the fabric passes from the strain-protected regions into the matrix (Fig. 5a). In other thin sections, S_2 and S_3 cleavages are both well-developed in the matrix, but S_3 is deformed and deflected by narrow zones of intensified S_2 cleavage (Fig. 6a).

Kinematic interpretation

Similar microstructures as described above have been described elsewhere by Bell (1986, fig. 5) and interpreted to indicate reactivation and extension of an early cleavage during a subsequent deformation event. See the Appendix for an outline of the reactivation concept and the resulting microstructures. At Hercules, post- or syn-D_3 shear movements along the S_2 cleavage are indicated by the above described deflection of S_3 into zones of intensified and reactivated S_2 (Fig. 6a). The movement sense is reverse, indicated by the sense of curvature of S_3 into S_2 and by offset veinlets. This shear sense is antithetic with respect to synthetic shear along S_3 crenulation limbs, in the context of being located on the east limb of a D_3 macroscopic antiform (see Appendix), thus consistent with reactivation of S_2 during D_3 folding (Bell, 1986). The reactivated S_2 cleavage is referred to as the "S_{2r3} cleavage" (S_2 reactivated during D_3).

The geometry of mesoscopic folds, which rapidly die out along their axial plane, is also consistent with progressive unfolding due to bedding anisotropy-induced shearing (Fig. 7). These folds have the dominant cleavage as axial plane and are therefore interpreted as F_2 folds. No macroscopic F_3 closures were recognized. Parasitic F_2 folds and F_3 crenulations have the same asymmetry and both are believed to have been partially destroyed by reactivation of S_2. This does not imply that wherever S_3 is not developed it was destroyed by reactivation of S_2. It is also possible that in large areas, particularly in competent zones, S_3 never did develop and S_2 was immediately reactivated at the onset of D_3 deformation.

Orebody-Host Rock Relationships

A surface map combining trace lines of bedding and cleavage juxtaposed on a projection of the orebody was produced to study the structural position of the ore (Fig. 3a). Because most of the ore occurs near the surface, the ore lenses were projected to surface along their dip direction from a series of 100-ft-spaced, east-west cross sections by Lees (1987) from drill core information and early underground mapping. Ore up to 25 m deep was projected to the surface, because at deeper levels the structural map pattern may deviate significantly from that observed at the surface and the distribution of mineralization may not bear any relationship to the structural pattern at the surface.

The map (Fig. 3a) shows the ore lenses discordant to folded bedding, as observed by previous workers (Hall et al., 1954, 1965). It further shows that the ore lenses parallel the axial planes of F_2^0 folds, which trend slightly more north-south than the main reactivated S_{2r3} cleavage (Fig. 3a-c). The apparent dips of the ore lenses and the dominant cleavage (S_{2r3}) are oblique in cross section (Fig. 4a), with the cleavage dipping slightly steeper. An explanation for the small angle between the dominant S_{2r3} cleavage on the one hand and the ore lenses and the F_2 hinge surfaces on the other is given in a later section.

Outcropping ore lenses were observed to be directly associated with parasitic F_2 folds in the field (Fig. 4b). The interpretative cross section (Fig. 4a) shows localization of ore lenses in the short limb zones of F_2 folds, based on the structural pattern observed at the surface and all available bedding orientation data on old mine level plans. Although, the proposed structural position of the ore in parasitic folds is largely interpretative, it satisfactorily explains the strata-bound, en echelon arrangement of ore lenses (Figs. 2 and 3a) and the parallel trends of ore lenses and F_2^0 folds. On the map (Fig. 3a), the projections of ore lenses do not always coincide with fold hinges. This could be due to the disharmonic character of folds and their limited continuity along their axial plane direction (Figs. 4a and 7). It is also possible that some fold hinges were almost completely obliterated by sulfide, leaving these only partially

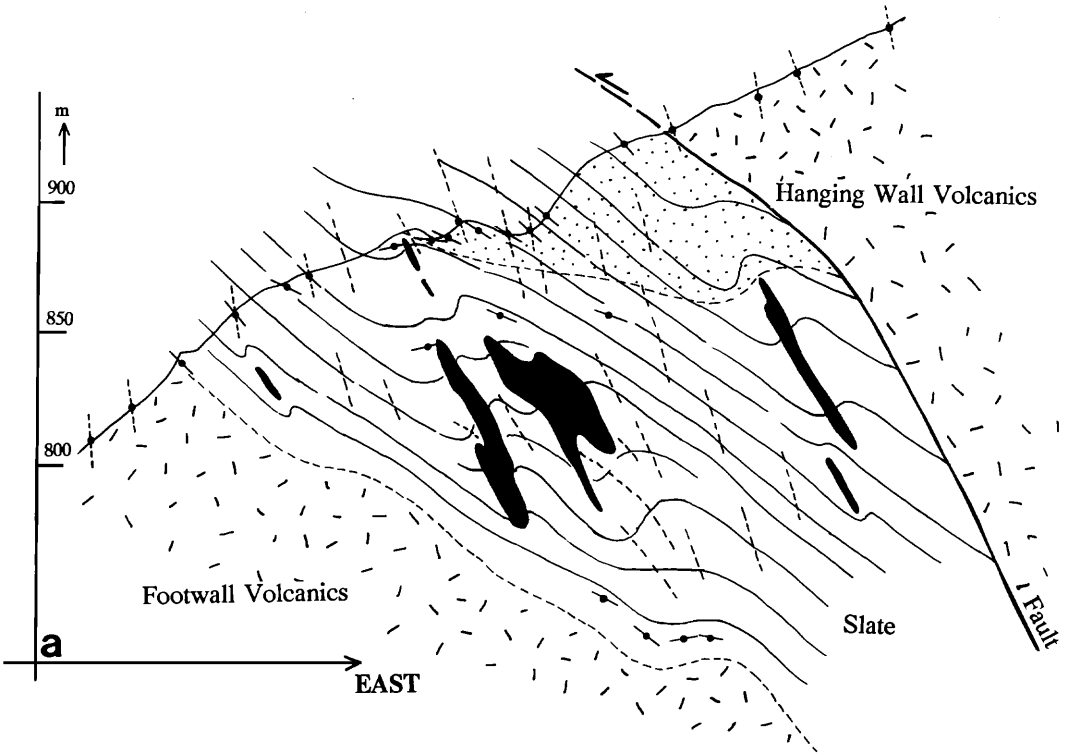

FIG. 4. a. Interpretation of the host-rock structure around the orebody on an east-northeast–west-southwest cross section based on the surface data of Figure 3a and all the available underground data from mine plans (on-section data represented by orientation symbols). Figure 3a shows position of the cross section (continuous lines = bedding; dashed lines = dominant cleavage S_{2r3}). The stippled area is the Black Slate unit as it appears in previous mine sections, based on drill core logging, not on structure. The

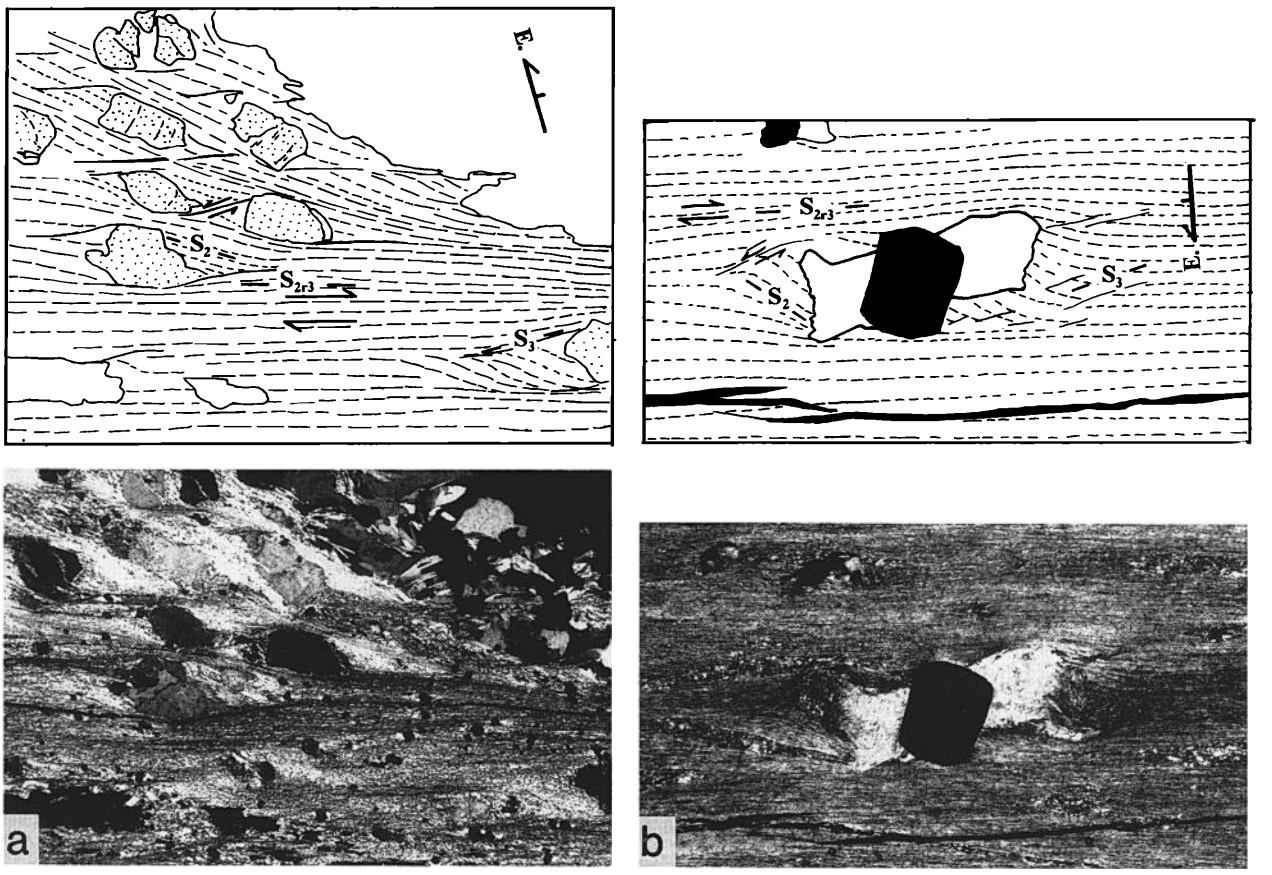

FIG. 5. a. Tracing (top) and photomicrograph (bottom) of a dextral, reactivated shear along S_2 during D_3 which caused destruction of S_3 and rotation of S_2 to a steeper orientation. In the strain shadows of the volcanic quartz crystals, S_2 retained a less steep orientation and S_3 is preserved. Reactivation of S_2 was antithetic to the (sinistral) shearing along S_3, deduced from the sense of curvature of S_3^2 crenulation limbs into the S_{2r3} cleavage. (Vertical east-west section; large half-arrow symbol marks east, horizontal, and up; see also Appendix and Fig. 17d and e; width of photomicrograph 2.1 mm). b. Tracing (top) and photomicrograph (bottom) of S_2 which was reactivated late during D_3 except in the strain shadows where S_3 is preserved and S_2 has a less steep orientation, as where it reactivated (S_{2r3}). Note the slight curvature of the pressure fringes on pyrite toward their ends, suggesting the pyrite grains grew during late D_2 deformation.

preserved above and below the ore lens (cf. Bell et al., 1988; Bell, 1991).

Timing and Genetic Interpretation

Timing of disseminated pyrite

Disseminated pyrite grains and grain aggregates occur throughout the mine area with quartz-chlorite pressure fringes. The fringes at Hercules are generally parallel to S_3 or S_{2r3} and the pyrite grains truncate the S_2 cleavage (Fig. 5b). However, some small pyrite grains were observed with slightly sigmoidal pressure fringes (Fig. 5b), possibly recording some extension during D_2 as well. Other pyrite grains are without any pressure fringes and sharply truncate both the S_2 and S_3 cleavage seams.

In the immediate vicinity of the orebody, locally higher concentrations of relatively large, euhedral py-

fact that the lower Black Slate boundary does not accord with the mapped bedding structure is because a large part of the host rock was not previously recognized as a highly altered equivalent of the Black Slate (see text). b. Traced photograph of the outcropping small ore lens shown in (a) just below the surface (mirror image to have same viewing direction as (a)). Bedding is obliterated by intense alteration immediately adjacent to the ore (black), but above it, a short limb zone of an F_2 fold is observed (fold axes average horizontal). The dashed line approximately separates what looks like Black Slate (left) from host-rock tuffs (location coordinates: 5,366,700 mN, 376,680 mE, Australian map grid; see hammer on loose block below massive ore for approximate scale).

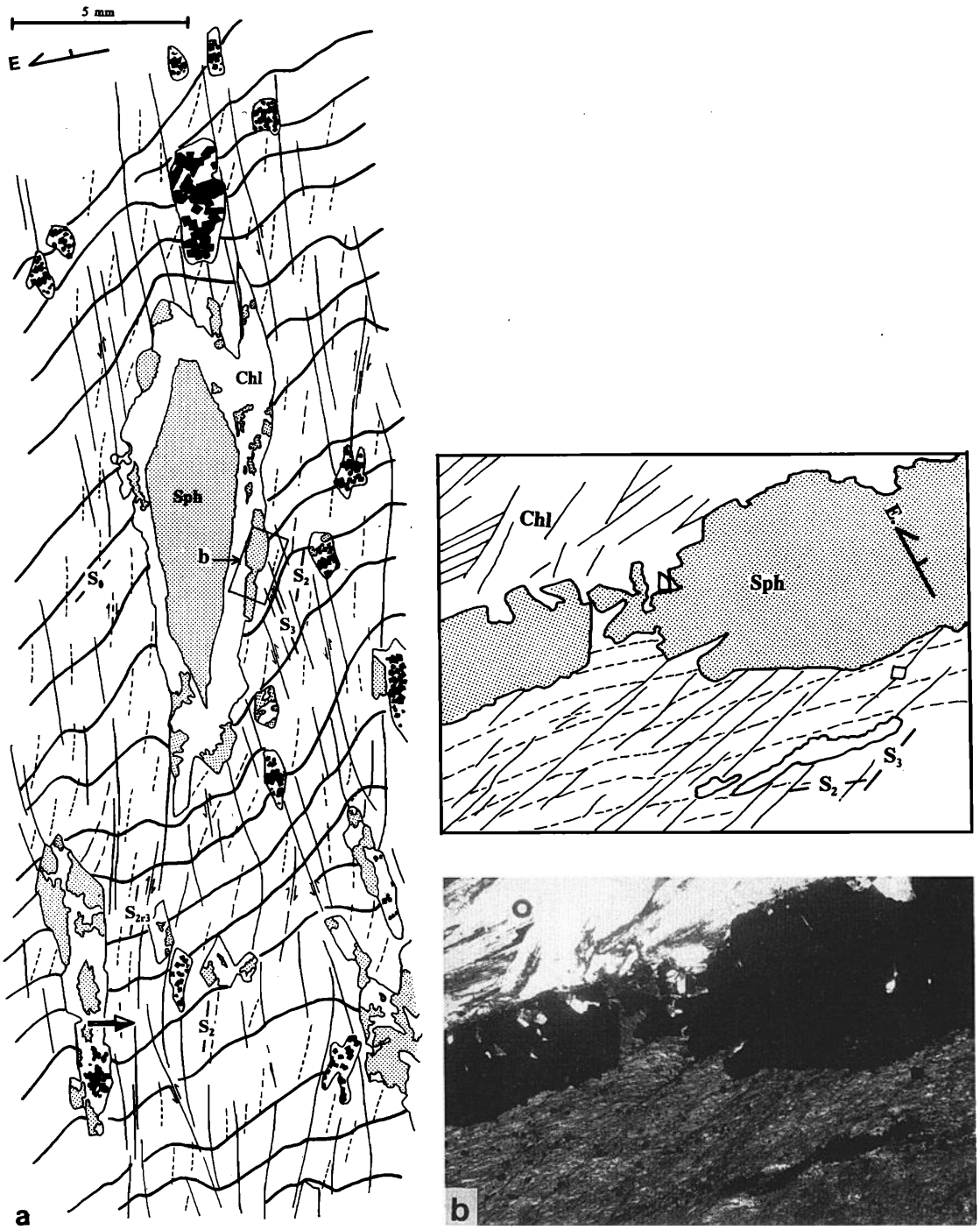

FIG. 6. a. Tracing of a thin section showing patches of sphalerite (Sph)-chlorite (Chl) mineralization in a matrix of chlorite schist. The two large mineralization patches are localized in F_2 short limbs. The mineralization sharply truncates bedding, S_2, and S_3. The S_2 and S_3 cleavages interfere in an anastomosing pattern, which is ascribed to the partial reactivation of S_2 during D_3. Reactivation is indicated by S_3 being locally dragged into zones of intensified S_2, labeled S_{2r3} (see arrow). Note the rhomb shape of the larger patch, controlled by the orientation of S_2 and/or S_3. b. Tracing (top) and photomicrograph (bottom) of a detail of (a) (area indicated) showing the abrupt truncation of S_3 and S_2 cleavages against the sphalerite-chlorite assemblage and indicating replacement of deformed host rock (base of photomicrograph 1.7 mm). Metasomatic chloritization (associated with sulfides) was to some extent controlled by the preexisting matrix fabric as indicated by preferential orientations of chlorite 001 planes, parallel to predating cleavages in the matrix.

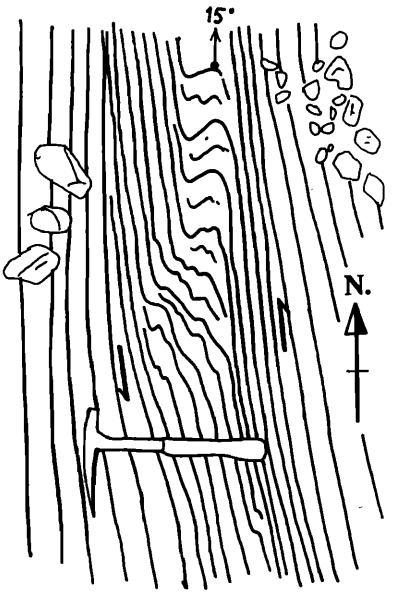

FIG. 7. The geometry of this F_2^0 fold observed at the surface at Hercules in a horizontal plane is interpreted as indicating that antithetic S_0-parallel shearing occurred after the fold developed. The fold plunges 15° N (arrow). See Appendix section for explanation (approximate Australian map grid coordinates: 5,366,220 mN, 376,750 mE).

rite crystals (0.5–1 mm) were found with variably developed pressure fringes parallel to S_3 and S_{2r3}. However, many extensional pyrite margins, or portions of these, apparently never did detach from the matrix as they sharply truncate the S_{2r3} cleavage (Fig. 8a and b). High concentrations of tiny pyrite euhedra (0.5–5 μ) occur next to the larger pyrite crystals and align along S_3 cleavage seams, locally aggregating into very thin, continuous pyrite seams. Composite pressure fringes also developed; they contain significant quantities of sphalerite, galena, and/or chalcopyrite along earlier contacts between large pyrite crystals and their silicate pressure fringes.

The above observations are consistent with prolonged pyrite growth, from early to late or even post-D_3 deformation. Some pyrite grains record D_2 deformation and are clearly pre-D_3 deformation (see above). These latter grains could have formed at any time before D_3 deformation and be either volcanogenic, diagenetic (pre-D_2), or syn-D_2 deformation. The base metal sulfides in composite pressure fringes appear to have nucleated syn-D_3 at preexisting pyrite-silicate fringe contacts, where they grew by replacement of the silicate fringe and possibly some replacement of the pyrite as well (Fig. 9).

Timing of patchy ore

The massive sulfide mineralization at Hercules comprises sphalerite, galena, pyrite, chalcopyrite, quartz, carbonate, chlorite, some barite, and white mica. The abundance ratios of these minerals are variable. In fact, massive, coarse-grained carbonate-silica pods (mm-m scale), which occur within the host rock can be regarded as sulfide-poor, gangue-rich equivalents of the ore lenses. Texturally, the ore assemblages have a granoblastic, undeformed appearance with typical grain sizes between 0.05 to 0.5 mm (Fig. 10a-c).

In the transition from unmineralized host rock to massive ore, elongate sphalerite-rich patches develop parallel to S_3 or S_{2r3} and sharply cut across F_2^0 microfolds in the matrix (Figs. 6a and 11a). The sim-

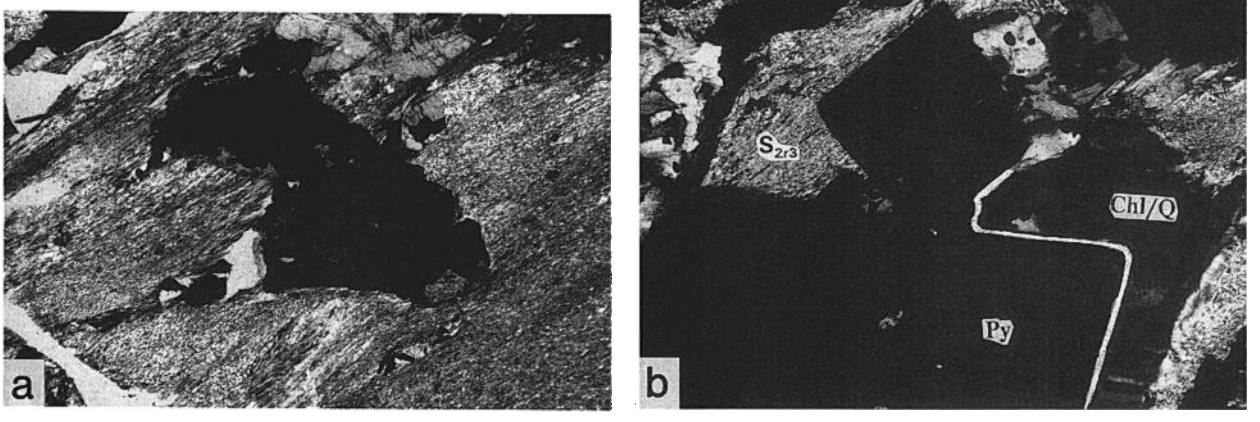

FIG. 8. a. Undeflected S_{2r3} cleavage is sharply truncated against pyrite grain, indicating that the grain overgrew the cleaved matrix. After overgrowth, small pressure fringes still developed on parts of the pyrite margins, indicating syntectonic growth (width of photomicrograph 2.1 mm). b. A portion of strongly cleaved host rock is enclosed and truncated by large pyrite grains. Continued extension after pyrite (Py) growth resulted in quartz (Q)-chlorite (Chl) being deposited at extensional pyrite margins (width of photomicrograph 1.1 mm).

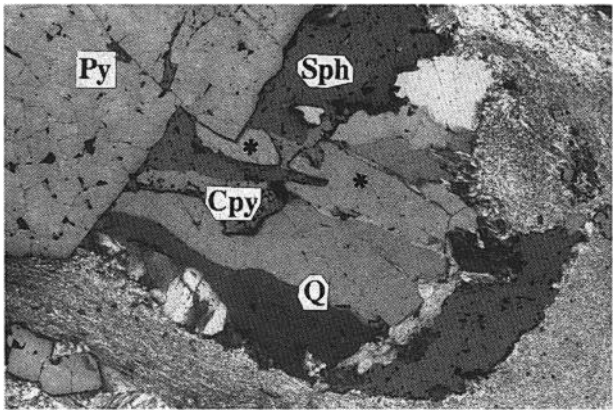

FIG. 9. Composite, metasomatic pressure fringe at a pyrite margin. Microfractures at an extensional pyrite matrix contact initially resulted in the formation of a quartz fringe, by an unspecified combination of microfracture infill and replacement of the microfracture wall. Subsequent fracturing at the quartz (Q)-pyrite (Py) contact allowed replacement of quartz by sphalerite (Sph) and chalcopyrite (Cpy). Quartz relicts with identical crystallographic orientation are marked with an asterisk. (crossed polarizers; width of photomicrograph 1.7 mm).

plest form of these patches is a sphalerite-rich core with an irregular rim of quartz, chlorite, or white mica, although lesser amounts of the same sulfides also exist outside the silicate zone. Partial replacement of the silicate rims by the sphalerite core is suggested by isolated silicate inclusions that have an identical optical orientation as relatively large grains with a corroded appearance along the leading sulfide front. These two-dimensional inclusions are interpreted as relicts of the incompletely replaced larger grains (Fig. 12a and b; compare with texture in Fig. 10a). It must be borne in mind that the inclusions as observed in two dimensions might be connected to the larger grain or to each other in the third dimension. However, the relevance of the microstructures presented is the total erratic geometry of the phase boundary with convex ingressions of one mineral into the other. Such phase boundary geometries generally do not result from equilibrium (re)crystallization of two phases (e.g., Stanton, 1972) but are more typical of reaction or replacement fronts.

Pyrite, chalcopyrite, and/or galena may be present in minor quantities at sphalerite-silicate boundaries and show similar replacement of the silicates as described for the sphalerite. Corrosion textures of euhedral pyrite cubes by surrounding base metal sulfides suggest that the latter grew slightly later in the paragenetic sequence.

The relatively coarse-grained chlorite, quartz, and white mica rims commonly show a weak pattern of outward radiating grains that obliterates delicate F_3^2 crenulations in the adjacent matrix (Figs. 6b and 11a). Nevertheless, S_3 and S_2 directions may be weakly preserved within the silicate rim, probably due to preferential nucleation and growth in preexisting crenulation hinge regions and mimetic overgrowth (Fig. 6b).

Geometric considerations: The distribution of mineralization along the axial planes of F_2^0 folds such that it crosses the folded layering could, in principle, be interpreted in two ways. Either discordant pretectonic mineralization was subsequently flattened parallel to the cleavage, or mineralization grew by syn- or post-tectonic replacement and was controlled by the

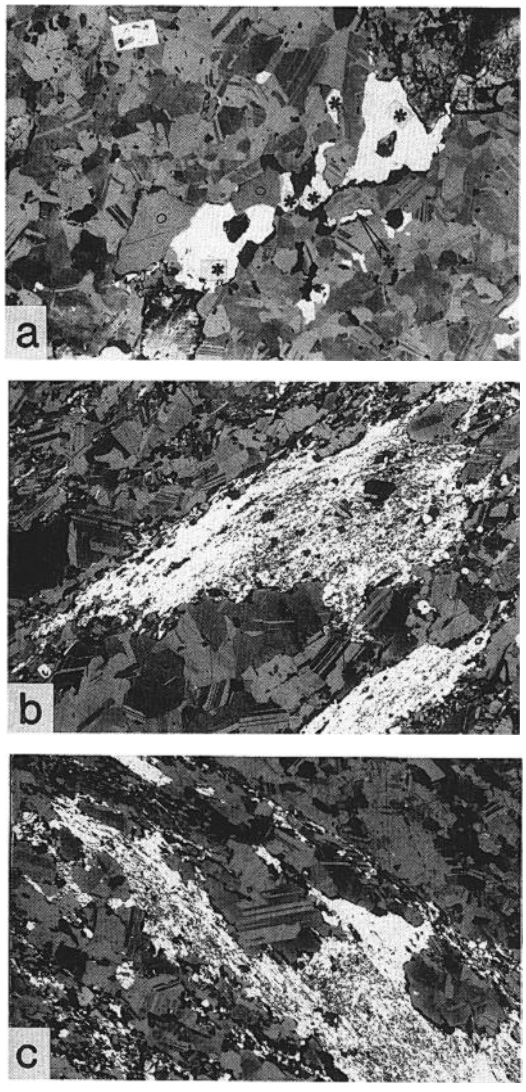

FIG. 10. a. Replacement of two quartz grains by massive sphalerite is indicated by the identical optical orientation of grouped quartz inclusions, at least in two dimensions (marked with corresponding symbols) and the erratic nature of the sulfide-quartz contacts (width of photomicrograph 2.5 mm). b. and c. Relict inclusions of intensely cleaved host rock. Replacement is indicated by the sharp truncation of the S_{2r3} cleavage by the highly irregular massive sphalerite front without evidence for deformation of the sulfide-host rock boundary. The sphalerite is undeformed and shows extensive growth twinning.

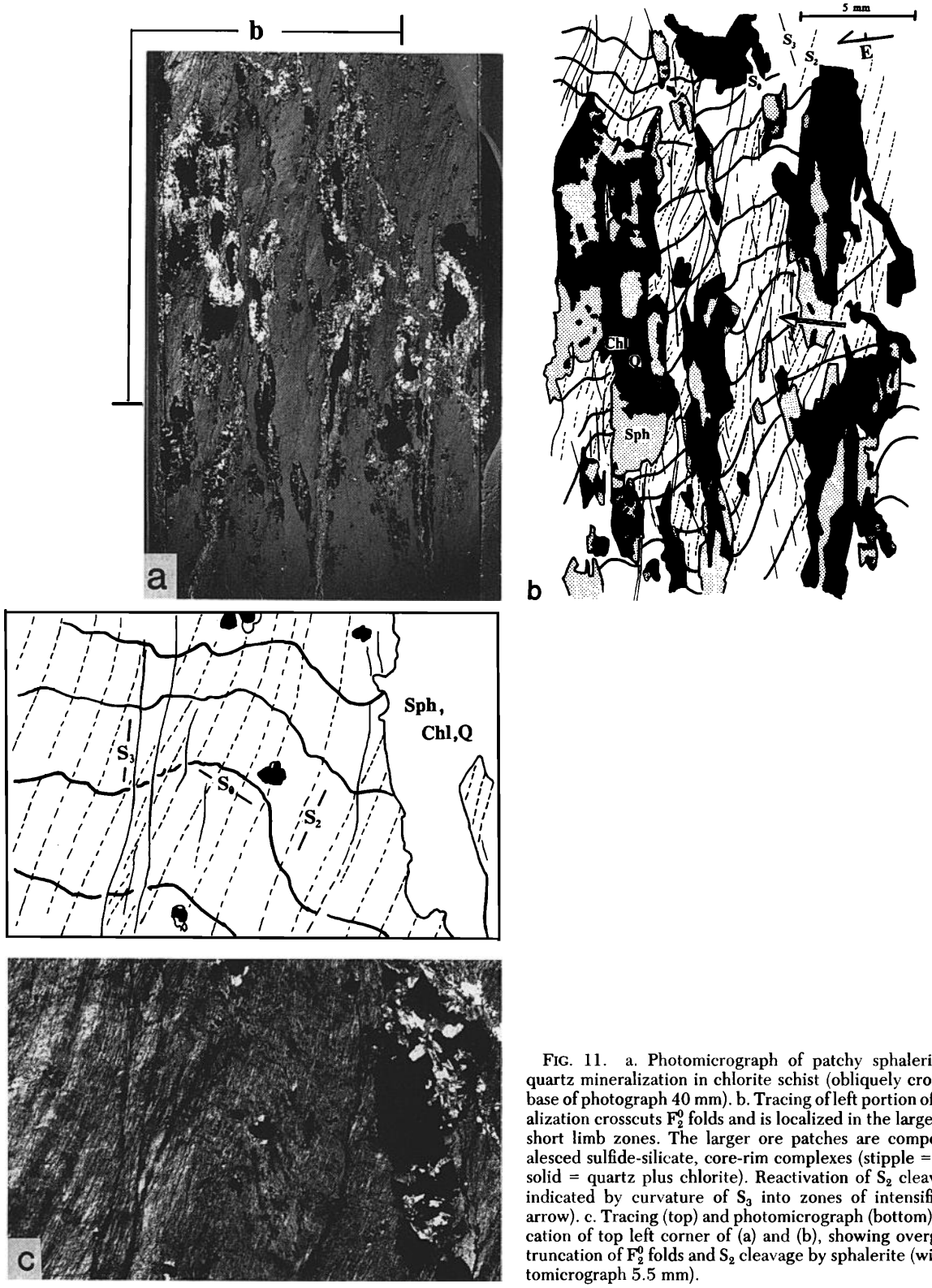

FIG. 11. a. Photomicrograph of patchy sphalerite-chlorite-quartz mineralization in chlorite schist (obliquely crossed nicols; base of photograph 40 mm). b. Tracing of left portion of (a). Mineralization crosscuts F_2^0 folds and is localized in the largely replaced short limb zones. The larger ore patches are composed of coalesced sulfide-silicate, core-rim complexes (stipple = sphalerite, solid = quartz plus chlorite). Reactivation of S_2 cleavage is also indicated by curvature of S_3 into zones of intensified S_2 (see arrow). c. Tracing (top) and photomicrograph (bottom) of magnification of top left corner of (a) and (b), showing overgrowth and truncation of F_2^0 folds and S_2 cleavage by sphalerite (width of photomicrograph 5.5 mm).

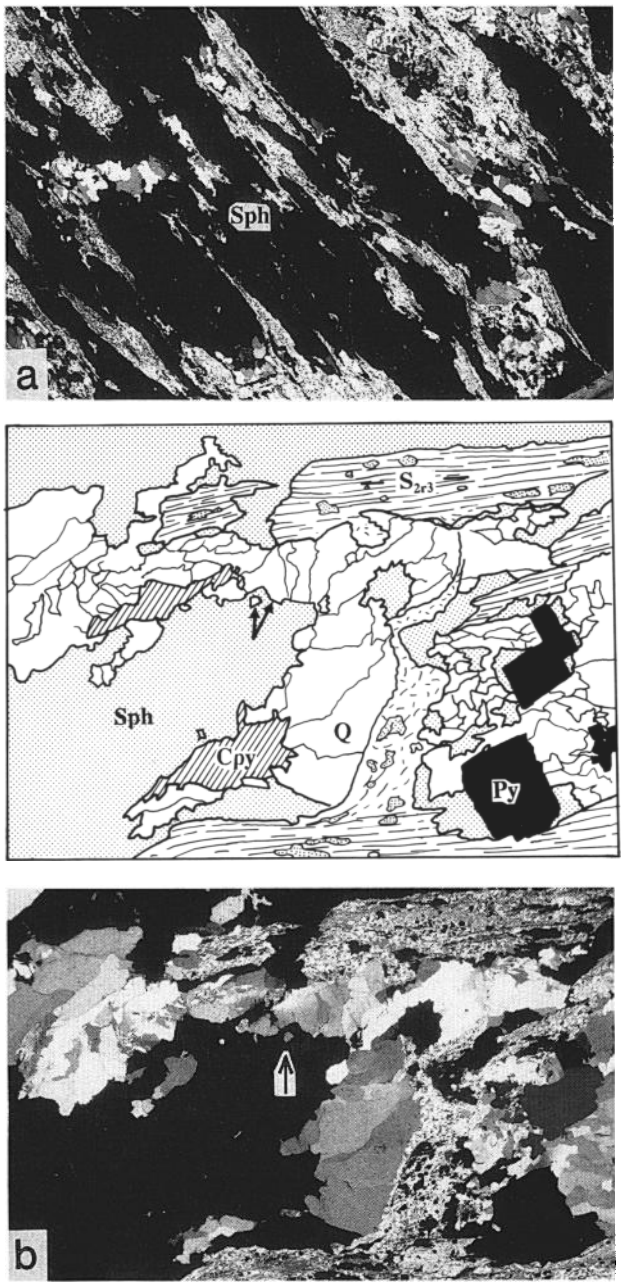

FIG. 12. a. Advanced replacement of sericite schist by sphalerite plus quartz along cleavage. The schist has been partially incorporated within the massive mineralization. Internal cleavages of these host-rock inclusions are truncated by both the sphalerite and the quartz (width of photomicrograph 18 mm). b. Tracing (top) and photomicrograph (bottom) of a detail from the right bottom corner of (a), showing replacement of an outer quartz (Q) rim by an inner sphalerite (Sph)-chalcopyrite (Cpy) zone containing relict inclusions of quartz. The optical orientation of such inclusions shows that they are derived from partially replaced larger quartz grains, commonly preserved at the leading replacement front (arrows). The S_{2r3} cleavage in these inclusions of host rock are sharply crosscut by the mineralization fronts. Note that sphalerite grew in the pressure shadows of paragenetic pyrite grains (right bottom corner; width of photomicrograph 5.5 mm).

axial plane of the F_2^0 folds. The second interpretation is favored because:

1. The elongate geometry of mineralization, subparallel to cleavage, would require intense deformation if one assumes that the mineralization is pretectonic (Figs. 6a, 11a, and 12a). Yet open folds in the matrix suggest only moderate deformation. This means that the deformation would have to be concentrated in the sulfides. However, if this were the case, strong deformation-partitioning effects, such as cleavage intensification and bedding rotating into parallelism with cleavage, should occur along the margins of the mineralization. In fact, the opposite is observed; bedding is truncated by the sulfides and neither the intensity nor the orientation of cleavage is affected by geometrically erratic, crosscutting ore contacts, regardless of the degree of mineralization (Figs. 6b and 11b–c). This strongly suggests late syn- or post-D_3 overprinting of the host-rock cleavages by the sulfides (cf. Aerden, 1992).

2. Neither sulfide nor silicate components of the mineralization show evidence of internal deformation. Annealing or dynamic recrystallization of the sulfide minerals, commonly held responsible for the lack of deformation microstructures in ores, could explain the generally uncleaved nature of the ore. However, preservation of intricate replacement geometries between sulfide and silicate components and the highly irregular nature of internal phase boundaries (Fig. 10a–c) are inconsistent with intense deformation of the ore, regardless of whether or not intramineralic annealing occurred. Intense deformation would have flattened and smoothed primary contacts between mineral phases with different competencies.

3. The rhombic shape of some zoned patches and the angular geometry of the matrix-mineralization contacts, which generally follow matrix-cleavage directions, strongly suggest a combined control of S_3 and S_2 on the localization of mineralization (Figs. 6a–b and 11a–c).

Timing of massive ore

Transitional into the massive ore zone, sulfide patches gradually coalesce, forming more complex zonal patterns, and the matrix is progressively reduced to relict inclusions in massive ore assemblages (compare Figs. 6a, 11a, 12a, and 13a). Individual coalesced patches can, in some cases, still be recognized by the way remains of silicate gangue and host rock are distributed. The massive base metal sulfides have irregular invading contacts into the host-rock inclusions as well as into relicts of paragenetically earlier metasomatic minerals (coarse-grained quartz, carbonate, and pyrite gangue). Replacement of the

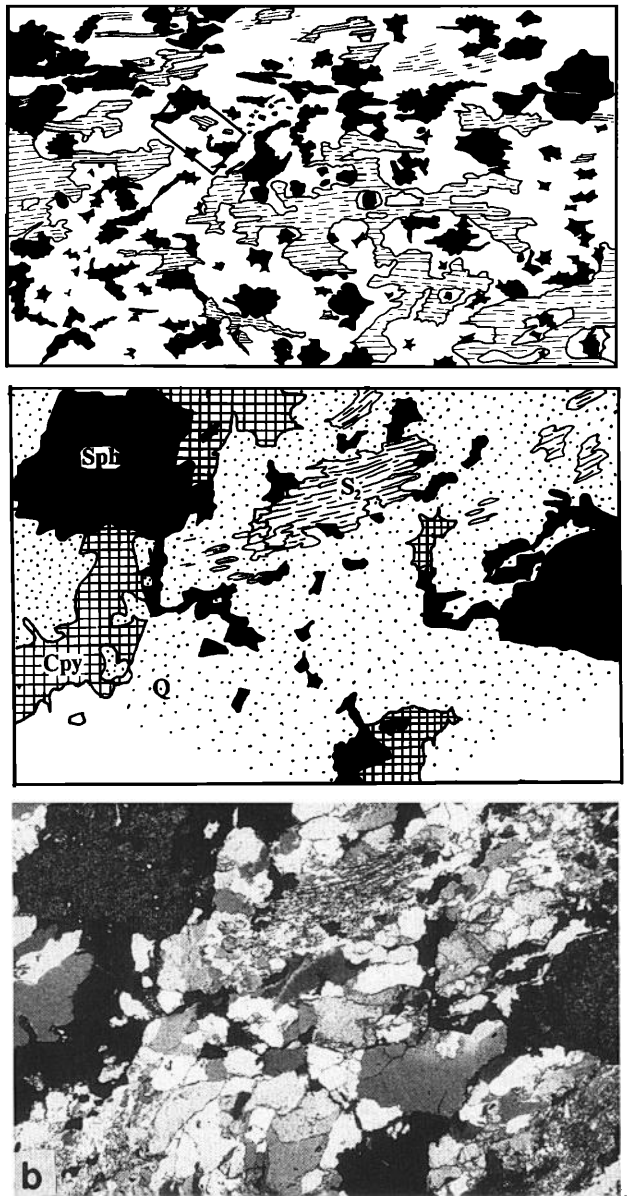

FIG. 13. a. Semimassive mineralization by sphalerite, galena, and chalcopyrite (solid), associated with coarse-grained quartz gangue (blank) that contains relict cleaved matrix (cleavage indicated by dashed thin lines; length of photograph 3.2 cm). b. Tracing (top) and photomicrograph (bottom) of detail of boxed area in (a), showing massive sphalerite-chalcopyrite-quartz mineralization that truncates the internal cleavage of a relic host-rock fragment (width of photomicrograph 4.2 mm).

latter is again indicated by the identical optical orientation of several grouped inclusions with highly irregular margins, suggestive of corrosion by the sulfide assemblage (Fig. 10a).

The massive sulfide mineralization contains abundant irregular relict inclusions of host rock whose internal cleavages are sharply truncated by erratic mineralization fronts, without any evidence for deformation of these contacts (Fig. 10b and c). This texture suggests that the mineralization formed late syn- or post-D_3, because deformation of irregular boundaries between materials of different competence can be expected to have a smoothing effect on these contacts by shearing off or flattening any irregularities. One would also expect intensification and wrapping of cleavage around protrusions of the more competent material into the softer material. However, neither of these relationships was observed. Instead, both the S_{2r3} and S_3 cleavages are truncated and undeflected at the mineralization fronts, and the erratic front geometry suggests that the host rock was progressively replaced. Cleaved matrix inclusions occur both in high-grade (sphalerite-rich) ore and in gangue-dominated assemblages (Figs. 10b–c and 13a–b).

A complete gradation occurs from composite or sphalerite pressure fringes growing off single pyrite grains, to patchy and semimassive mineralization, to massive pyrite-quartz-sphalerite mineralization containing relict host rock. All these degrees of mineralization show similar replacement relationships, which yield the following paragenetic sequence: pyrite → quartz plus chlorite → carbonate → late-stage pyrite → sphalerite, plus galena, plus chalcopyrite. This sequence is also found in the Rosebery ore deposit (Aerden, 1991, 1992). The above therefore suggests a syn-D_3 timing of all the mineralization types at Hercules.

Microstructural control on mineralization

In thin section, mineralization appears to be preferentially localized in the short limb zones of F_2^0 microfolds. The axial plane cleavage (S_2) of these folds is crosscut at a small angle by S_3. The degree of reactivation of S_2 to form S_{2r3} commonly varies at the scale of a thin section and can be measured from the amount of rotation of S_3 toward S_{2r3}. Simultaneous operation of synthetic shear parallel to S_3 and antithetic shear along S_{2r3} is indicated by S_2 curving into zones of intense S_3 and zones of intense S_{2r3}, dragging the S_3 into them in the same thin section. S_3- and S_{2r3}-dominated tracts thereby enclose rhomb-shaped domains of lower strain (Figs. 6a and 11a).

The localization of the ore patches in short limb zones can be rationalized in terms of preferential fracturing and dilation in these structural domains, thereby allowing fluid infiltration and metasomatic replacement. Concentration of brittle deformation in F_2^0 short limb zones could result from the high angle of bedding to the direction of maximum bulk extension in these zones during the D_3 folding event (Fig. 14a). This could then lead to a pulling apart of individual bedding layers as their orientation could not favor accommodation of folding by bedding-parallel shear.

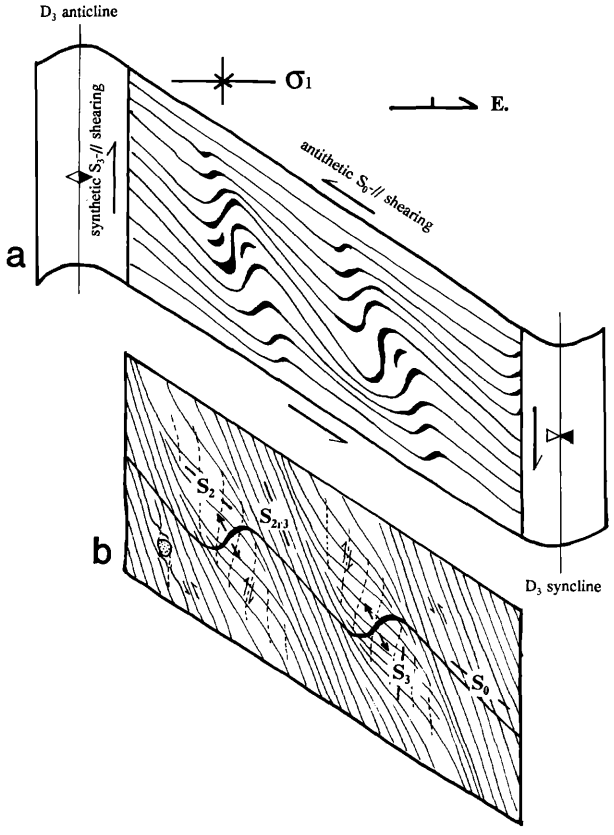

FIG. 14. a. Diagram explaining how dilatancy could be induced in parasitic F_2 folds during antithetic shear along bedding. The short limbs fracture and pull apart because they are at a high angle to the bulk extension direction (see also Fig. 17b). b. The attitude of S_2, S_{2r3}, and S_3 in the same volume of rock as shown in (a). The short limb zones oppose reactivation of S_2, which therefore remains crenulated and undergoes less rotation. Antithetic shearing in the long limb zones decrenulates S_2, and steepens S_0 and S_2. In this way S_{2r3} is at an angle to the short limb zones and S_2.

Bedding in the long limb zones, on the other hand, could occupy the extensional quadrant of the bulk instantaneous, stretching axes. It could therefore accommodate D_3 folding by antithetic layer-parallel shearing and would require no fracturing (see Appendix). This scenario would lead to a progressively decreasing angle between S_{2r3} and the long limbs, whereas in the short limbs bedding would retain a more stable orientation at a high angle to S_2 (Fig. 14b and Appendix Fig. A1e). A higher angle between S_2 or S_{2r3} and bedding in the short limbs is exactly what is observed in thin section (Figs. 6a, 11b, and 15).

The geometry of replacement domains in thin section commonly reflects a combined control by S_3 and S_{2r3}. In zones of intense S_2 reactivation, low strain pods containing the short limbs of F_2 folds are narrow and confined between zones of intense S_{2r3}. Preferential mineralization of such domains could lead to elongate ore patches parallel to S_{2r3} (Fig. 15). In zones of moderate reactivation, deformation would proceed by a combination of shearing along the S_3 and S_{2r3} cleavages. Bedding in these areas generally would preserve a higher angle with the S_{2r3} cleavage and low strain pods would be enclosed by both S_{2r3} and S_3 cleavage planes. Selective mineralization of such low strain pods in some cases led to almost perfect lozenge-shaped mineralization patches as shown in Figure 6b.

As already suggested, base metal sulfides generally form the center of mineralization patches and replace the inner margin of the surrounding silicate gangue. This pattern suggests that the host rock became replaced across two telescoping replacement fronts; an outer front leading a zone of replacement by silicates, closely followed by a sulfide replacement front. Sulfides at the margins of mineralization patches can be explained as the latest stages of mineralization nucleating at matrix-mineralization contacts with orientations at a high angle to the principle extension direction (Figs. 11b and 15).

FIG. 15. Sphalerite-chlorite-quartz mineralization in low strain domains, confined between zones of intense reactivation of S_2 and S_0. In the low strain zones, S_0 and S_2 have a less steep orientation and S_3 is preserved (see host rock at the extremities of the ore patches). It is envisaged that these sites were preferentially replaced as they microfractured and boudinaged between the zones of ductile shearing. Replacement of these sites is supported by the uncleaved nature of the mineralization and truncation of S_2 and S_3 cleavages. The ore patches are roughly zoned with a silicate rim and sphalerite core, suggesting that they are individual replacement aggregates and not elongate, transposed portions of pre-D_3 ore.

Macrostructural control

The microstructural evidence presented above indicates that the Hercules ore formed syn-D_3 and was, at least on a small scale, localized by parasitic F_2 folds. The bedding selectively gaped in these domains during D_3 folding. Macroscopically, an identical structural position of the ore in the short limb zones of F_2 folds is suggested (Figs. 3 and 4a–b). Consequently, the same mechanism of fracturing-controlled mineralization is invoked. The model predicts an angle between the axial planes of F_2^0 folds (and S_2 cleavage) and the S_{2r3} cleavage outside the fold area (Fig. 14b). This was observed in thin section and is also expressed macroscopically in the slightly different dips and strikes of ore lenses and F_2 fold trends, versus the regionally dominant S_{2r3} cleavage (Figs. 3a and 4a).

At Hercules, bedding in the host rock is closely spaced and gaping of bedding in the short limb zones is thought to have led to localized increased permeability. I suggest that the lens-shaped mineralization domains parallel to cleavage, rather than bedding-parallel mineralization in a discrete number of isolated tension gashes, express the tract of generally increased permeability. Recent studies of orebodies attributed to syntectonic replacement have also concluded that mineralization was commonly controlled by zones of fracturing and brecciation, related to hydrothermal fluid infiltration and evidenced by reaction with the immediate wall rock (e.g., Bell and Cuff, 1989). Examples of different structural controls documented in massive sulfide replacement deposits are (1) unfolding and gaping of a discordant lithologic contact during folding (Mount Isa, Queensland; Bell et al., 1988), (2) fold-hinge dilation during folding (Elura mine, New South Wales; de Roo, 1989; Haile mine, North Carolina; Hayward, 1992), (3) discordant lithologic contacts across thrusts, and (4) large-scale foliation boudinage in a high strain zone (Rosebery; Aerden, 1991). Gaping on such macroscopic anisotropy planes caused a sudden release of fluid pressure and rockburst in the immediately adjacent wall rock. This produced zones of pervasive microfracturing around the gape that could be selectively replaced (e.g., Hobbs, 1987; Bell et al., 1988).

Discussion

Pretectonic versus syntectonic ore genesis

Syntectonic mineralization overprinting primary massive sulfide deposits is commonly formed by local dissolution, fluid transfer, and redeposition of ore into (replacement) veins. Consequently, it could be argued that at Hercules partial dissolution of primary sulfides was followed by redeposition of the dissolved sulfides as replacements of wall rock along the original boundaries of the (primary) orebody. Timing of mineralization based on the host rock-ore contacts would falsely suggest replacement of host-rock schist by the entire orebody, instead of by a marginal fringe of remobilized mineralization.

Against this possibility at Hercules is the continuous transition from syntectonic patches of mineralization to massive ore with identical paragenetic textures (Fig. 16). There is no textural evidence for a segregation into primary and secondary ore components or for mineralization by a process other than replacement of schistose sediments. This strongly suggests that the scale is the only difference between ore patches in hand specimens and the ore lenses. In contrast to this, remobilized sulfides can generally be distinguished from their source material by a different texture and/or composition and occur in highly localized zones of low strain or fracturing (Gilligan and Marshall, 1987). Also, the cleavage-parallel margins in the Hercules orebody would be expected to be sites of dissolution instead of redeposition. The formation of a continuous fringe of remobilized material around a precursor orebody is therefore highly unlikely. There is no evidence either for a nearby pretectonic orebody that could have been the main source for the Hercules orebody. Consequently the favored model at Hercules involves large-scale dissolution of disseminated sulfides, focused upward migration, and concentration in structural traps.

Volcanogenic models at Hercules are believed to be inconsistent with the microstructural evidence for syntectonic replacement throughout the orebody. They are also difficult to reconcile with the macro-

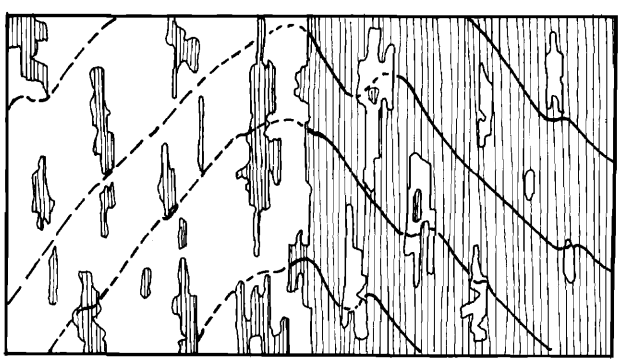

FIG. 16. Schematic illustration of the transition from patchy ore to massive ore (white) containing relics of host rock. At Hercules all these mineralization types show the same paragenetic replacement textures and sharply truncate cleavages in the host rock (thin lines). Bedding is indicated by the solid lines; replaced bedding by a dashed line. Note that the relicts of host rock within the massive ore are shown to be controlled by small-scale short limbs within the larger scale short limb represented by the right half of the diagram. These small-scale short limbs have the same orientation as the larger scale long limbs (east dipping), at a low angle to the bulk extension direction, which inhibits fracturing apart from beds. The drawing is purely speculative because bedding was generally not observed within the relicts of host rock.

scopic geometry of the orebody. A number of hypothetical models are considered below.

The discordant nature of ore lenses has been ascribed by some to mechanical remobilization of sedimentary sulfide lenses (Corbett and Lees, 1987). Similar processes have been widely applied in other deposits (e.g., Sangster, 1979). Nevertheless, where mechanical remobilization by ductile flow of sulfides into zones of dilation has been demonstrated, generally involved relatively small portions of a larger primary orebody. Complete, solid state mobilization of the ore, without any traces of the primary (concordant) material remaining, is highly unlikely (Gilligan and Marshall, 1987) and not supported by any evidence at Hercules. Such a process would most likely also have involved intricate folding of the primary stratigraphic orebody zoning, but previous mine geologists have reported simple downdip mineralogical trends within individual ore lenses (e.g., Lees, 1987). Almost identical downdip mineralogical zoning has been described in syntectonic massive sulfide lodes in Wales (Phillips, 1972).

Perhaps a more viable pretectonic model would be mineralization formed as isolated, subsurface replacement bodies. Such bodies could initially have had any shape but assuming a roughly equidimensional shape, their present lens geometry (aspect ratios of 1/5–1/15 common) would indicate extreme flattening. This is contradicted by the structure of the immediately enveloping host rock showing a high angle between bedding and cleavage. Concentration of deformation in the ore would most likely have resulted in a narrow shear zone affecting bedding above and below the ore lens. This is not observed and, in fact, the ore is localized in fold hinge regions, which are generally zones of relatively low strain compared to the limbs of folds. Also, some massive quartz-carbonate alteration lenses exhibit identical structural relationships, despite having a higher competency than the surrounding rock as indicated by slight cleavage wrapping. Obviously, if the attenuation of these bodies was due to deformation, the immediately surrounding host rock should have been extremely deformed and isoclinally folded.

The most viable pretectonic model, therefore, envisages a number of discordant replacement bodies that formed primarily with a tabular shape. The association with F_2 fold hinges could then be attributed to a mechanism of fold nucleation on the ore lenses, assuming these behaved as relatively competent bodies. This model would be consistent with the lack of internal deformation of the ore and the preserved internal paragenetic replacement relationships. However, apart from the microstructural evidence that mineralization overprints the cleavage, this model encounters two problems. First, there is no evidence for any pervasively developed, pretectonic fracture set or foliation in the host rock. This would be required to control ore deposition in tabular bodies on all scales. Second, it would be highly coincidental if such a pre-D_2 fabric would exactly overlap with the regional S_2 cleavage that developed subsequently.

Stratigraphic control on orebodies

Although small massive sulfide replacement veins occur in shear zones stratigraphically above and below the Hercules slate horizon (e.g., Ring P. A. and east Hercules prospects), by far the largest concentrations of sulfides in the Rosebery-Hercules district occur close beneath or within a well-layered slate horizon. This fact has been used to support sedimentary exhalative ore formation at a specific stratigraphic level. However, the association of the orebodies with this stratigraphic unit is also expected in a syntectonic replacement model. A thin slate layer surrounded by massive volcanics is likely to accommodate regional deformation by concentrating shear strain within it. A second potential role of the slate units is as relatively impermeable barriers, allowing fluid pressure to build up below. This would enhance fracturing, dilation, and hence, mineralization (Phillips, 1972; Sibson, 1981; Etheridge et al., 1983, 1984; Hobbs, 1987; Bell et al., 1988).

Source and transport of material

Pb isotope data suggest that the sulfides comprising the Cu-Pb-Zn mineralization in the Mount Read Volcanics are distinctly older than the tin-tungsten mineralization from, for example, the Renison-Bell mine, which is clearly related to Devonian granite intrusions (Gulson and Porritt, 1987). Aerden (1991, 1992, in prep.) suggested that this age difference could reflect different sulfide sources rather than different times of orebody emplacement. He suggested that Cambrian sulfides within the Mount Read Volcanic pile were dissolved and migrated upward during cleavage formation and metamorphism until they were concentrated by reprecipitation in structural traps. Such a concentration process would not necessarily have altered the Pb and S signature of the Cambrian source material (cf. Solomon et al., 1987).

Transport toward sites of deposition may have involved a combination of focused, upward fluid flow and elemental diffusion through interconnecting fractures and fluid films (Hobbs, 1987). The latter process is generally considered less important, although Bell and Cuff (1989) have recently argued that the rate of diffusion along phyllosilicate domains of active cleavages could be orders of magnitude greater than the rates that have been experimentally measured for passive, solid state diffusion. Although this concept needs experimental verification, it could account for the recorded volume losses in deformed

rocks and the upward transport of large amounts of material without needing the unrealistically high fluid-rock ratios and many cycles of fluid recirculation against lithostatic pressure gradients in the fluid required by Etheridge et al. (1983, 1984). Transport by diffusion would also explain the lack of extensive fracture systems below both the Rosebery and Hercules orebodies, which would be expected if material was transported purely by fluid advection (cf. Bell and Cuff, 1989).

Eastoe et al. (1987) and Green (1990) defined a broad zone of high Mg chlorite and low δ^{18} isotope values in the footwall to the deposit. They believed that this mineralization occurred in the Cambrian. However, focused hydrothermal fluid flow directed toward the location of the orebody could also have produced this alteration pattern during Devonian metamorphism. Perhaps detailed mapping of the geochemical zoning could provide further proof for the timing of mineralization and alteration relative to regional folding. The $\delta^{18}O$ values (Green, 1990) are consistent with the Cambrian seawater-hydrothermal fluid-mixing hypothesis, but they are also consistent with a metamorphic fluid which was not in equilibrium with the volcanics but generated elsewhere in the crust (i.e., from outside the volcanics). The $\delta^{18}O$ data do not preclude a metamorphogenic origin for the Hercules deposit.

Massive sulfides in the Mount Read Volcanics

A Devonian replacement origin of the Rosebery and Hercules orebodies contrasts with a volcanogenic origin for other massive sulfide deposits in the Cambrian Mount Read Volcanics. Interpretation of these deposits relies heavily on tentative prefolding reconstructions of ore geometry and regional and mine-scale geochemical zoning patterns; the timing of mineralization relative to matrix microfabrics has only been superficially considered (Brathwaite, 1969; Cox, 1981; Green et al., 1981; Large et al., 1988; Zaw et al., 1990). Isotope data are consistent with volcanogenic sulfides but not inconsistent with a syntectonic origin of mineralization (Aerden, 1991, 1992). Therefore, microstructural timing and detailed studies of the structural relationships between the ores and their host rocks are necessary to verify or reject a Cambrian origin.

Conclusions

Sulfide mineralization and alteration occurred by the metasomatic replacement of slate during D_3 in the Devonian. A syn- or post-D_3 timing of mineralization is indicated by the overgrowth on S_2 and S_3 and the gradual incorporation of replacement relics of host rock in the massive sulfides and associated silicate gangue. Slight anastomosing of S_{2r3} around gangue-rich pods and the occurrence of pressure shadows on early mineralization further constrains the timing of mineralization to late syn-D_3. Replacement was controlled by localized dilation and fracturing between beds in short limb zones of parasitic F_2 folds. Paragenetic replacement relationships indicate the following replacement sequence: early pyrite → {quartz, chlorite} → late pyrite → {sphalerite, galena, chalcopyrite}. Isotope data are consistent with the sulfides at Hercules and Rosebery, derived from the Mount Read Volcanics through synmetamorphic leaching, upward transport, and structurally controlled concentration at higher crustal levels.

Acknowledgments

This study was undertaken as part of a Ph.D. project at the James Cook University of North Queensland. It was funded by a James Cook University scholarship. I would like to thank T. H. Bell for his valuable supervision. I acknowledge generous logistic support from Pasminco Mining, Rosebery. M. Hinman, R. Keele, T. Lees, B. Marshall, and two *Economic Geology* reviewers suggested important improvements to the manuscript. I kindly thank M. Quayl for collecting some additional rock specimen.

May 23, 1990; September 28, 1992

REFERENCES

Aerden, D. G. A. M., 1991, Foliation boudinage control on the formation of the Rosebery Pb-Zn orebody, Tasmania: Jour. Struct. Geology, v. 13, p. 759–755.

—— 1992, Macro and microstructural controls on the genesis of the Rosebery and Hercules Pb-Zn ore deposits, western Tasmania: Unpub. Ph.D. thesis, Townsville, Australia, James Cook Univ. North Queensland, 260 p.

Allen, R. L., and Cas, R. A. F., 1990, The Rosebery controversy: Distinguishing prospective sub-marine ignimbrite-like units from true subaerial ignimbrites in the Rosebery-Hercules Zn-Cu-Pb massive-sulphide district [abs.]: Australian Geological Convention, 10th, Hobart, February 1990, Abstracts, p. 31–32.

Bell, T. H., 1986, Foliation development and refraction in metamorphic rocks: Reactivation of earlier foliations and decrenulations due to shifting patterns of deformation partitioning: Jour. Metamorphic Geology, v. 4, p. 421–444.

—— 1991, The role of thrusting in the structural development of the Mount Isa mine and its relevance to exploration in the surrounding region: ECON. GEOL., v. 86, p. 1602–1625.

Bell, T. H., and Cuff, C., 1989, Dissolution, solution transfer, diffusion vs fluid flow and volume loss during deformation/metamorphism: Jour. Metamorphic Geology, v. 7, p. 425–447.

Bell, T. H., and Johnson, S. E., 1992, Shear sense: A new approach that resolves conflicts between criteria in metamorphic rocks: Jour. Metamorphic Geology, v. 10, p. 99–124.

Bell, T. H., Perkins, W. G., and Swager, C. P., 1988, Structural controls on development and localization of syntectonic copper mineralization at Mount Isa, Queensland: ECON. GEOL., v. 83, p. 69–85.

Brathwaite, R. L., 1969, The geology of the Rosebery ore deposit: Unpub. PhD. thesis, Univ. Tasmania, 218 p.

Burton, C. C. J., 1975, Rosebery, Hercules and Mt. Farrell mines: Melbourne, Australasian Inst. Mining Metallurgy Mon. 5, p. 619–626.

Choukroune, P., 1971, Contribution à létude des mécanismes de

la déformation avec schistosité grâce aux crisytallisations syncinématiques dans les "zones abritées" ("pressure shadows"): Soc. Géol. France Bull., 7, v. 13, p. 257–271.
Collins, P. L. F., and Williams, E., 1986, Metallogeny and tectonic development of the Tasman fold belt system in Tasmania: Ore Geology Rev., v. 1, p. 153–201.
Corbett, K. D., 1981, Stratigraphy and mineralization in the Mount Read Volcanics, western Tasmania: ECON. GEOL., v. 76, p. 209–230.
—— 1986, The geological setting of mineralisation in the Mt Read Volcanics, *in* Large, R. R., ed., The Mount Read Volcanics and associated ore deposits: Hobart, Geol. Soc. Australia, Tasmania Div., p. 1–10.
Corbett, K. D., and Lees, T. C., 1987, Stratigraphy and structural relationships and evidence for Cambrian deformation at the western margin of the Mt. Read Volcanics, Tasmania: Australian Jour. Earth Sci., v. 34, p. 45–67.
Corbett, K. D., Solomon, M., McClenaghan, M. P., Carswell, J. T., Green, G. R., Iliff, G., Howarth, J. W., McArthur, G. J., and Wallace, D. B., 1989, Cambrian Mt Read Volcanics and associated minerals deposits: Geol. Soc. Australia Spec. Pub., v. 15, p. 84–153.
Cox, S. F., 1981, The stratigraphic and structural setting of the Mt. Lyell volcanic-hosted sulfide deposits: ECON. GEOL., v. 76, p. 231–245.
Eastoe, C. J., Solomon, M., and Walshe, J. L., 1987, District-scale alteration associated with massive sulfide deposits in the Mount Read Volcanics, western Tasmania: ECON. GEOL., v. 82, p. 1239–1258.
Etheridge, M. A., Wall, V. J., and Vernon, R. H., 1983, The role of the fluid phase during regional metamorphism and deformation: Jour. Metamorphic Geology, v. 1, p. 205–226.
Etheridge, M. A., Wall, V. J., Cox, S. F., and Vernon, R. H., 1984, High fluid pressure during regional metamorphism and deformation; implications for mass-transport and deformation mechanisms: Jour. Geophys. Research, v. 89, p. 4344–4358.
Gilligan, L. B., and Marshall, B., 1987, Textural evidence for remobilization in metamorphic environments: Ore Geology Rev., v. 2, p. 205–229.
Green, G. R., 1983, The geological setting and formation of the Rosebery volcanic hosted massive sulphide ore body, Tasmania: Unpub. Ph.D. thesis, Univ. Tasmania, 288 p.
—— 1986, Stable isotope and alteration investigations of the Mount Read Volcanics I - The Hercules and Boco areas, in Large, R. R., ed., The Mount Read Volcanics and associated ore deposits: Hobart, Geol. Soc. Australia, Tasmania Div., p. 1–10.
—— 1990, Rock alteration, mineral and oxygen isotope zonation in the Rosebery district, Tasmania [abs.]: Australian Geological Convention, 10th, Hobart, February 1990, Abstracts, p. 15.
Green, G. R., Solomon, M., and Walshe, J. L., 1981, The formation of the volcanic-hosted massive sulfide ore deposit at Rosebery, Tasmania: ECON. GEOL., v. 76, p. 304–338.
Gulson, B. L., and Porritt, P. M., 1987, Base metal exploration of the Mount Read Volcanics, western Tasmania: Pt. II. Lead isotope signatures and genetic implications: ECON. GEOL., v. 82, p. 291–307.
Hall, G., Cottle, V. M., Rosenhain, P. B., and McGhie, R. R., 1954, Lead-zinc ore deposits of Read-Rosebery and Mt. Farrell, *in* Edwards, A. B., ed., Geology of the Australian ore deposits, 1st ed.: p. 1145–1159.
Hall, G., Rosenhain, V. N., McGhie, R. R., and Druett, J. G., 1965, Lead zinc ore deposits of Read-Rosebery, in McAndrew, J., ed., Geology of Australian Ore Deposits, 2nd ed.: p. 485–489.
Hayward, N., 1992, Controls of syntectonic replacement mineralization in parasitic antiforms, Haile gold mine, Carolina slate belt: ECON. GEOL., v. 87, p. 91–112.
Hendry, D. A. F., 1981, Chlorites, phengites and siderites from the Prince Lyell ore deposit, Tasmania, and the origin of the deposit: ECON. GEOL., v. 76, p. 285–303.
Hobbs, B. E., 1987, Principles involved in mobilization and remobilization: Ore Geology Rev., v. 2, p. 37–45.
Johnson, S. E., 1990, Deformation history of the Otago schists, New Zealand, from progressive developed porphyroblast/matrix microstructures: Cyclic uplift-collapse orogenesis and its implications: Jour. Struct. Geology, v. 12, p. 727–746.
Large, R. R., McGoldrick, P. J., Berry, R. F., and Young, C. H., 1988, A tightly folded, gold-rich, massive sulfide deposit: Que River mine, Tasmania: ECON. GEOL., v. 83, p. 681–693.
Lees, T., 1987, Geology and mineralization of the Rosebery Hercules area: Unpub. M.Sc. thesis, Univ. Tasmania.
Markham, N. L., 1968, Some genetic aspects of the Mt Lyell mineralisation: Mineralium Deposita, v. 3, p. 199–221.
McLeod, R. L., and Stanton, R. L., 1984, Phyllosilicates and associated minerals in some Paleozoic stratiform sulfide deposits of southeastern Australia: ECON. GEOL., v. 79, p. 1–22.
Phillips, W. J., 1972, Hydraulic fracturing and mineralization: Geol. Soc. London Jour., v. 128, p. 337–359.
Roo, de, J. A., 1989, The Elura Ag-Pb-Zn mine in Australia—ore genesis in a slate belt by syndeformational metasomatism along hydrothermal fluid conduits: ECON. GEOL., v. 84, p. 256–278.
Sibson, R. H., 1981, Fluid flow accompanying faulting: Field evidence and models: Am. Geophys. Union Maurice Ewing Ser., v. 4, p. 593–603.
Solomon, M., 1981, An introduction to the geology and metallic ore deposits of Tasmania: ECON. GEOL., v. 76, p. 194–208.
Solomon, M., Rafter, T. A., and Jensen, M. L., 1969, Isotope studies on the Rosebery, Mount Farrell and Mount Lyell ores, Tasmania: Mineralium Deposita, v. 4, p. 172–199.
Solomon, M., Vokes, F. M., and Walshe, J. L., 1987, Chemical remobilization of volcanic hosted sulphide deposits at Rosebery and Mt. Lyell, Tasmania: Ore Geology Rev., v. 2, p. 173–190.
Solomon, M., Eastoe, C. J., Walshe, J. L., and Green, G. R., 1988, Mineral deposits and sulfur isotope abundances in the Mount Read Volcanics between Que River and Mount Darwin, Tasmania: ECON. GEOL., v. 83, p. 1307–1328.
Stanton, R. L., 1972, Ore petrology: New York: McGraw Hill, 713 p.
Walshe, J. L., and Solomon, M., 1987, An investigation into the environment of formation of the volcanic-hosted Mount Lyell copper orebody, using geology, mineralogy, stable isotopes, and a six-component chlorite solid solution model: ECON. GEOL., v. 76, p. 246–284.
Zaw, K., Large, R. R., and Huns, S., 1990, Geology and geochemistry of the precious metal-rich south Hercules volcanogenic sulphide deposit [abs.]: Australian Geological Convention, 10th, Hobart, February 1990, Abstracts.

APPENDIX

Cleavage Reactivation during Folding

When an early foliation is folded, two shearing systems are commonly competing: synthetic shearing along the actively forming crenulation cleavage (e.g., S_3) and antithetic, anisotropy-induced shearing along the foliation being folded (e.g., S_2; Choukroune, 1971; Bell, 1986; Johnson, 1990; Fig. A1a). "Reacti-

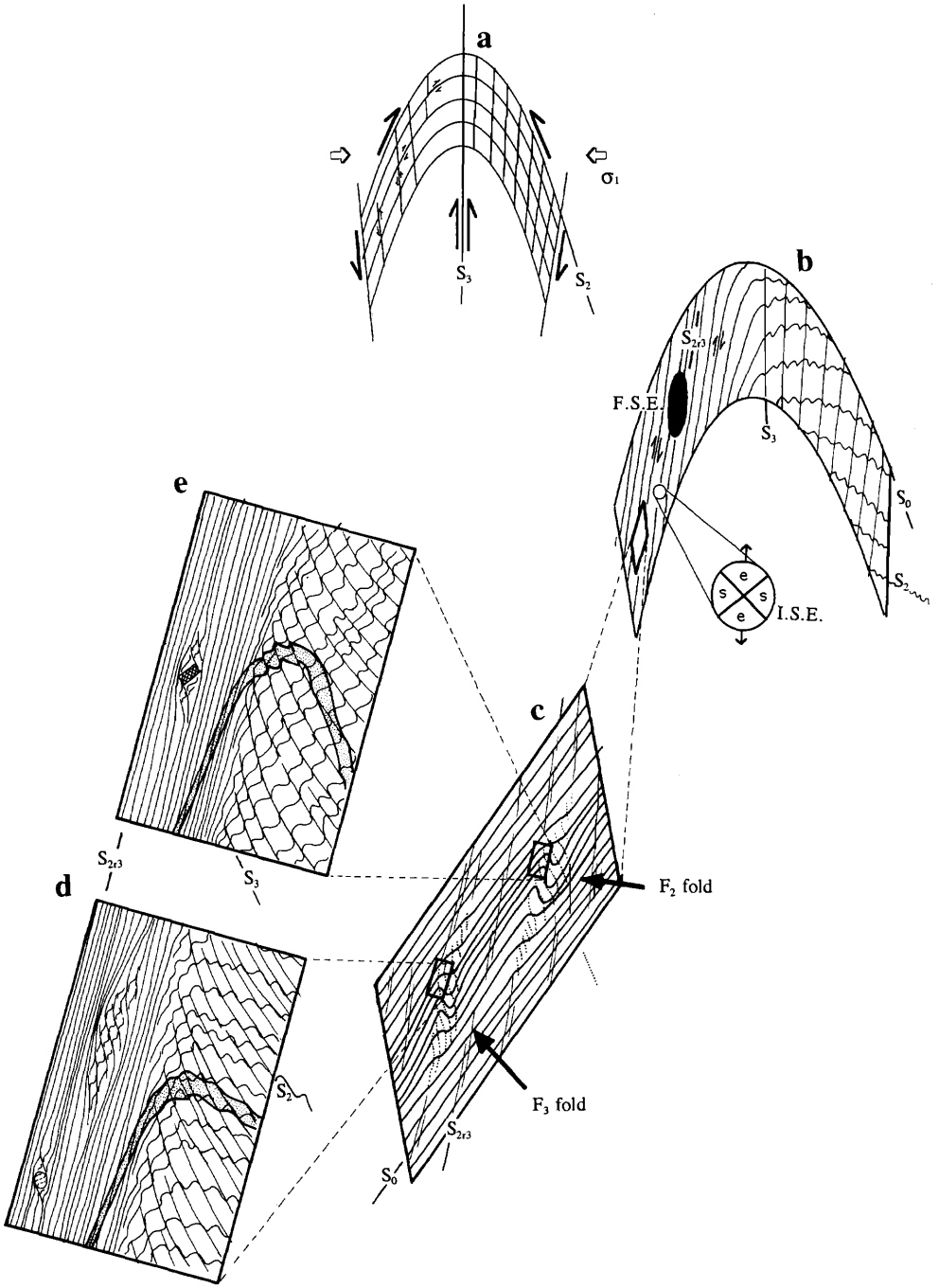

FIG. A1. a. and b. The concept of bedding-controlled reactivation of a hypothetic cleavage S_1 during a subsequent deformation event D_2 is illustrated. c. Parasitic F_1 and F_2 folds within the left-hand fold limb of (b). d and e. (Unoriented) details of the upper parts of the F_2 and F_1 folds in (c), respectively. The role of rigid objects and low strain pods as preservers of prereactivation fabrics is also illustrated. See text for explanation.

vation" of a foliation (Bell, 1986) occurs when shearing along the actively forming foliation is arrested and deformation proceeds dominantly by antithetic shearing along the old foliation. This happens as the early foliation reaches a critical angle with respect to the bulk compression direction σ_1, after rotating into

the extensional field of the bulk instantaneous strain ellipsoid (ISE; Fig. A1b). Cleavage reactivation generally occurs on one fold limb only, as on the other limb the foliation lies in the shortening field of the ISE and is crenulated (Fig. A1b).

In bedded rocks, cleavage reactivation is commonly controlled by the bedding anisotropy, with different degrees of reactivation in different beds. Cleavage refraction from one layer to another is a clear expression of this (Bell, 1986). Within a certain bed, reactivation generally commences in narrow zones that progressively broaden out, thereby causing decrenulation and unfolding of (in the case of Hercules) F_3 crenulations and folds, which formed earlier during the same deformation event (Fig. A1c and d). Note from Figure A1c that in zones where reactivation occurs, the crenulation cleavage and the older cleavage rotate toward each other. The original orientations of these foliations are typically preserved in low strain zones and as inclusion trails in syntectonic porphyroblasts (Bell, 1986; Fig. A1d and e). Parasitic folds of an earlier deformation event (F_2) may also undergo unfolding if they have the same assymetry as the F_3 folds (Fig. A1e).